Journal of Applied Fluid Mechanics , Vol. 8, No. 3, pp. 351-365, 2015.
Available online at www.jafmonline.net, ISSN 1735-3572, EISSN 1735-3645.
DOI: 10.18869/acadpub.jafm.67.222.23471

The Influence of Heat Transfer on Peristaltic Transport of MHD Second Grade Fluid through Porous Medium in a Vertical Asymmetric Channel

K. Ramesh[1] and M. Devakar[1†]
[1]*Department of Mathematics, Visvesvaraya National Institute of Technology, Nagpur-440010, India.*

† *Corresponding Author Email*: *m_devakar@yahoo.co.in*

(Received June 20 2014; accepted July 04 2014)

Abstract

In this paper, we study the influence of heat transfer on the peristaltic transport of an incompressible magnetohydrodynamic second grade fluid in vertical symmetric and asymmetric channels. The channel asymmetry is produced by choosing the peristaltic wave train on the walls to have different amplitudes and phase. The flow is investigated in the wave frame of reference moving with velocity of the wave. Perturbation solutions are obtained for the stream function, temperature and pressure gradient under long wave length assumption. Pressure difference and frictional force are discussed through numerical integration. The influence of various parameters of interest on the flow are discussed and also the graphical results are obtained for different wave forms.

Keywords: Second grade fluid; Peristaltic transport; Porous medium; Magnetohydrodynamic flow; Heat transfer.

1. Introduction

Peristalsis is an important mechanism generated by the propagation of waves along the walls of a channel or tube. In the recent times, peristalsis has attracted much attention due to its important engineering and medical applications. It occurs like, chyme movement in the gastrointestinal tract, urine transport from kidneys to bladder through ureter, transport of spermatozoa in the ductus afferents of the male reproductive tracts, movement of ovum in the female fallopian tube, transport of bile in the bile duct, transport of cilia, circulation of blood in small blood vessels and many other glandular ducts in a living body. Recently, peristaltic flows in asymmetric channel have gained the attention of researchers working in this field. This is because the physiologists observed that the intrauterine fluid flow caused by myometrial contractions may occur in both symmetric and asymmetric directions (Nadeem and Akbar 2011). Some important studies describing the peristaltic flows in asymmetric channel are made in the references (Mishra and Rao 2003; Ali and Hayat 2008; Noreen *et al.* 2012; Rani and Sarojamma 2004).

Due to the extensive applications in bio engineering and medical sciences, in recent years, bio magnetic fluid dynamics is emerging as an interesting area of research. Few such applications include the development of magnetic devices for cell separation, cancer tumor treatment, reduction of bleeding during surgeries and development of magnetic tracers (Rathish and Naidu 1995; Hayat *et al.* 2007). Significant studies concerning the magnetohydrodynamic peristaltic transport have been made in (Hayat *et al.* 2007; Kothandapani and Srinivas 2008; Nadeem and Akbar 2010; Nadeem and Akram 2010; Nadeem and Akram 2011; Wang *et al.* 2009). Further more, flow through porous medium has attracted the attention of several researchers due to its practical applications in bio fluid dynamics. The porous medium is involved in the human lung, bile duct, gall bladder with stones and in small blood vessels (Afifi and Gad 2001). In view of this, several investigators (Elmaboud and Mekheimer 2011; Nadeem and Akram 2011; Shehawey and Husseny 2002; Vajravelu et al. 2012; Tripathi and Anwar 2012) have studied peristaltic flow problems through porous medium. The study of heat transfer on the peristaltic flow problems is also most important in many engineering as well as physiological applications. This mechanism may occur in obtaining information about properties of tissues, hypothermia treatment, sanitary fluid transport, blood pump in heart-lung machines and transport of corrosive fluids (Nadeem and Akram 2011). Some more works on this topic can be seen in (Nadeem and Akbar 2009; Hayat *et al.* 2011; Vajravelu *et al.* 2011; Srinivas and Kothandapani 2008; Hayat *et al* 2014; Mehmood *et al.* 2012; Saleem and Haider 2014; Tripathi and Anwar 2014).

Motivated from the previous studies, the aim of the present paper is to discuss the influence of heat transfer on peristaltic flow of a second grade fluid through a porous medium in two-dimensional vertical symmetric and asymmetric channels. The fluid is electrically conducted in the presence of a magnetic field. The governing equations of second grade fluid have been modeled in cartesian coordinates.

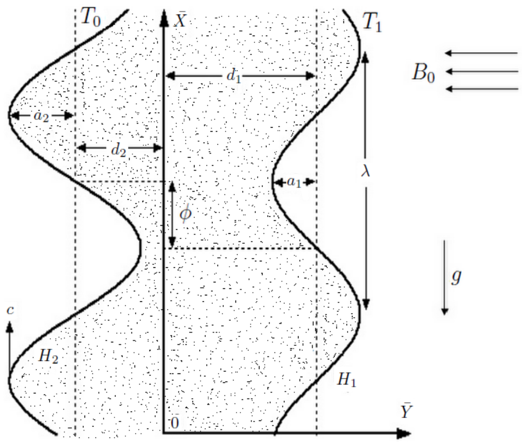

Fig. 1. Schematic diagram of the physical model.

2. Mathematical Formulation

Consider the peristaltic flow of an incompressible, electrically conducting second grade fluid in two dimensional vertical asymmetric channel through porous medium (see Figure 1). Asymmetry in the flow is due to the propagation of peristaltic waves of different amplitudes and phase on the channel walls. The heat transfer in the channel is taken into account. The left wall of the channel is maintained at temperature T_0, while the right wall has temperature T_1. We assume that the fluid is subject to a constant transverse magnetic field B_0. The magnetic Reynolds number is assumed to be small and hence the induced magnetic field can be neglected. In the laboratory frame, we select cartesian coordinate system in such a way that $\bar{X}$-axis lies along the center line of the channel and $\bar{Y}$-axis normal to it. We assume that, an infinite wave train is travelling with velocity c along the walls. The geometry of the wall surface is defined as

$$H_1\left(\bar{X},\bar{t}\right) = d_1 + a_1 \cos\left(\frac{2\pi}{\lambda}\left(\bar{X}-c\bar{t}\right)\right) \tag{1}$$

$$H_2\left(\bar{X},\bar{t}\right) = -d_2 - a_2 \cos\left(\frac{2\pi}{\lambda}\left(\bar{X}-c\bar{t}\right)+\phi\right) \tag{2}$$

In the above equations, a_1 and a_2 are the waves amplitudes, λ is the wave length, d_1+d_2 is the channel width, c is the velocity of propagation, $\bar{t}$ is the time and $\bar{X}$ is the direction of wave propagation. The phase difference ϕ varies in the range $0 \leq \phi \leq \pi$, in which $\phi = 0$ corresponds to symmetric channel with waves out of phase and $\phi = \pi$ corresponds to that with waves in phase, and further a_1, a_2, d_1, d_2 and ϕ satisfy the condition $a_1^2 + a_2^2 + 2a_1a_2\cos\phi \leq (d_1+d_2)^2$.

In laboratory frame, the equations governing the two-dimensional peristaltic motion of an incompressible magnetohydrodynamic second grade fluid through porous medium in the vertical channel are

$$\frac{\partial \bar{U}}{\partial \bar{X}} + \frac{\partial \bar{V}}{\partial \bar{Y}} = 0 \tag{3}$$

$$\rho\left(\frac{\partial}{\partial \bar{t}} + \bar{U}\frac{\partial}{\partial \bar{X}} + \bar{V}\frac{\partial}{\partial \bar{Y}}\right)\bar{U} = -\frac{\partial \bar{P}}{\partial \bar{X}} + \frac{\partial\left(\bar{S}_{\bar{X}\bar{X}}\right)}{\partial \bar{X}} + \frac{\partial\left(\bar{S}_{\bar{Y}\bar{X}}\right)}{\partial \bar{Y}} - \sigma B_0^2\bar{U} - \frac{\mu}{k}\bar{U} + \rho g\gamma(T-T_0) \tag{4}$$

$$\rho\left(\frac{\partial}{\partial \bar{t}} + \bar{U}\frac{\partial}{\partial \bar{X}} + \bar{V}\frac{\partial}{\partial \bar{Y}}\right)\bar{V} = -\frac{\partial \bar{P}}{\partial \bar{Y}} + \frac{\partial\left(\bar{S}_{\bar{X}\bar{Y}}\right)}{\partial \bar{X}} + \frac{\partial\left(\bar{S}_{\bar{Y}\bar{Y}}\right)}{\partial \bar{Y}} - \frac{\mu}{k}\bar{V} \tag{5}$$

$$\rho c_p\left(\frac{\partial}{\partial \bar{t}} + \bar{U}\frac{\partial}{\partial \bar{X}} + \bar{V}\frac{\partial}{\partial \bar{Y}}\right)T = k^*\left(\frac{\partial^2 T}{\partial \bar{X}^2} + \frac{\partial^2 T}{\partial \bar{Y}^2}\right) + Q_0 \tag{6}$$

where ρ is the density, $\bar{U}$ and $\bar{V}$ are the velocity components, σ is the electrical conductivity of the fluid, k is the permeability parameter and B_0 is the magnetic field. Introducing a wave frame $(\bar{x},\bar{y})$ moving with velocity c away from the fixed frame $(\bar{X},\bar{Y})$, the transformations

$$\bar{x} = \bar{X} - c\bar{t}, \quad \bar{y} = \bar{Y} \quad \text{give} \quad \bar{u} = \bar{U} - c, \quad \bar{v} = \bar{V},$$
$$\bar{p}(\bar{x},\bar{y}) = \bar{P}\left(\bar{X},\bar{Y},\bar{t}\right) \quad \text{and} \quad \bar{T}(\bar{x},\bar{y}) = T\left(\bar{X},\bar{Y},\bar{t}\right) \tag{7}$$

where $(\bar{u},\bar{v})$ and $(\bar{U},\bar{V})$ are velocity components, $\bar{p}$ and $\bar{P}$ are pressures, $\bar{T}$ and T are temperatures in wave and fixed frame of references respectively.
After employing Eq. (7), Eq.s (3)-(6) reduce to

$$\frac{\partial \bar{u}}{\partial \bar{x}} + \frac{\partial \bar{v}}{\partial \bar{y}} = 0 \tag{8}$$

$$\rho\left(\bar{u}\frac{\partial}{\partial\bar{x}}+\bar{v}\frac{\partial}{\partial\bar{y}}\right)\bar{u}=-\frac{\partial\bar{p}}{\partial\bar{x}}+\frac{\partial\left(\bar{S}_{\bar{x}\bar{x}}\right)}{\partial\bar{x}}+\frac{\partial\left(\bar{S}_{\bar{y}\bar{x}}\right)}{\partial\bar{y}} -\sigma B_0^2(\bar{u}+c)-\frac{\mu}{k}(\bar{u}+c)+\rho g\gamma(\bar{T}-\bar{T}_0) \quad (9)$$

$$\rho\left(\bar{u}\frac{\partial}{\partial\bar{x}}+\bar{v}\frac{\partial}{\partial\bar{y}}\right)\bar{v}=-\frac{\partial\bar{p}}{\partial\bar{y}}+\frac{\partial\left(\bar{S}_{\bar{x}\bar{y}}\right)}{\partial\bar{x}}+\frac{\partial\left(\bar{S}_{\bar{y}\bar{y}}\right)}{\partial\bar{y}} -\frac{\mu}{k}\bar{v} \quad (10)$$

$$\rho\left(\bar{u}\frac{\partial}{\partial\bar{x}}+\bar{v}\frac{\partial}{\partial\bar{y}}\right)\bar{T}=k^*\left(\frac{\partial^2\bar{T}}{\partial\bar{x}^2}+\frac{\partial^2\bar{T}}{\partial\bar{y}^2}\right)+Q_0 \quad (11)$$

Using the non-dimensional variables

$$x=\frac{\bar{x}}{\lambda},\quad y=\frac{\bar{y}}{d_1},\quad u=\frac{\bar{u}}{c},\quad v=\frac{\bar{v}}{c},$$
$$h_2=\frac{H_2}{d_1},\quad t=\frac{c\bar{t}}{\lambda},\quad S=\frac{d_1}{\mu c}\bar{S},\quad p=\frac{d_1^2}{\lambda\mu c}\bar{p},$$
$$\delta=\frac{d_1}{\lambda},\quad d=\frac{d_2}{d_1},\quad a=\frac{a_1}{d_1},\quad b=\frac{a_2}{d_1},$$
$$Re=\frac{\rho c d_1}{\mu},\quad \alpha_1=\frac{c\bar{\alpha}_1}{\mu d_1},\quad \alpha_2=\frac{c\bar{\alpha}_2}{\mu d_1},$$
$$M=\sqrt{\frac{\sigma}{\mu}}B_0 d_1,\quad D_a=\frac{k}{d_1^2},\quad \psi=\frac{\bar{\Psi}}{c d_1},$$
$$Pr=\frac{\mu c_p}{k^*},\quad Gr=\frac{\rho g\gamma d_1^2(\bar{T}_1-\bar{T}_0)}{\mu c},$$
$$h_1=\frac{H_1}{a_1},\quad \theta=\frac{\bar{T}-\bar{T}_0}{\bar{T}_1-\bar{T}_0},\quad \beta=\frac{Q_0 d_1^2}{k^*(\bar{T}_1-\bar{T}_0)}$$

in equations (8)-(11), we get

$$\delta\frac{\partial u}{\partial x}+\frac{\partial v}{\partial y}=0 \quad (12)$$

$$Re\delta\left(u\frac{\partial u}{\partial x}+\frac{1}{\delta}v\frac{\partial u}{\partial y}\right)=-\frac{\partial p}{\partial x}+\delta\frac{\partial\left(S_{xx}\right)}{\partial x} +\frac{\partial\left(S_{yx}\right)}{\partial y}-\left(M^2+\frac{1}{D_a}\right)(u+1)+Gr\theta \quad (13)$$

$$Re\delta^2\left(u\frac{\partial v}{\partial x}+\frac{1}{\delta}v\frac{\partial v}{\partial y}\right)=-\frac{\partial p}{\partial y}+\delta^2\frac{\partial\left(S_{xy}\right)}{\partial x} +\delta\frac{\partial\left(S_{yy}\right)}{\partial y}-\frac{\delta}{D_a}v \quad (14)$$

$$RePr\delta\left(u\frac{\partial\theta}{\partial x}+\frac{1}{\delta}v\frac{\partial\theta}{\partial y}\right)=\left(\delta^2\frac{\partial^2\theta}{\partial x^2}+\frac{\partial^2\theta}{\partial y^2}\right)+\beta \quad (15)$$

Introducing the dimensionless stream function $\psi(x,y)$ such that $u=\frac{\partial\psi}{\partial y}$ and $v=-\delta\frac{\partial\psi}{\partial x}$, the governing Eq.s (13)-(15) become

$$Re\delta\left[\left(\frac{\partial\psi}{\partial y}\frac{\partial}{\partial x}-\frac{\partial\psi}{\partial x}\frac{\partial}{\partial y}\right)\frac{\partial\psi}{\partial y}\right]=-\frac{\partial p}{\partial x} +\delta\frac{\partial\left(S_{xx}\right)}{\partial x}+\frac{\partial\left(S_{yx}\right)}{\partial y} -\left(M^2+\frac{1}{D_a}\right)\left(\frac{\partial\psi}{\partial y}+1\right)+Gr\theta \quad (16)$$

$$-Re\delta^3\left[\left(\frac{\partial\psi}{\partial y}\frac{\partial}{\partial x}-\frac{\partial\psi}{\partial x}\frac{\partial}{\partial y}\right)\frac{\partial\psi}{\partial x}\right]=-\frac{\partial p}{\partial y} +\delta^2\frac{\partial\left(S_{xy}\right)}{\partial x}+\delta\frac{\partial\left(S_{yy}\right)}{\partial y}+\frac{\delta^2}{D_a}\frac{\partial\psi}{\partial x} \quad (17)$$

$$RePr\delta\left(\frac{\partial\psi}{\partial y}\frac{\partial\theta}{\partial x}-\frac{\partial\psi}{\partial x}\frac{\partial\theta}{\partial y}\right)=\left(\delta^2\frac{\partial^2\theta}{\partial x^2}+\frac{\partial^2\theta}{\partial y^2}\right) +\beta \quad (18)$$

with

$$S_{xx}=2\delta\frac{\partial^2\psi}{\partial x\partial y}+\alpha_1\left[2\delta^2\frac{\partial\psi}{\partial y}\frac{\partial^3\psi}{\partial x^2\partial y} -2\delta^2\frac{\partial\psi}{\partial x}\frac{\partial^3\psi}{\partial x\partial y^2}+4\delta^2\left(\frac{\partial^2\psi}{\partial x\partial y}\right)^2 -2\delta^2\frac{\partial^2\psi}{\partial x^2}\frac{\partial^2\psi}{\partial y^2}+2\delta^4\left(\frac{\partial^2\psi}{\partial x^2}\right)^2\right] +\alpha_2\left[4\delta^2\left(\frac{\partial^2\psi}{\partial x\partial y}\right)^2+\left(\frac{\partial^2\psi}{\partial y^2}\right)^2 +\delta^4\left(\frac{\partial^2\psi}{\partial x^2}\right)^2-2\delta^2\frac{\partial^2\psi}{\partial x^2}\frac{\partial^2\psi}{\partial y^2}\right] \quad (19)$$

$$S_{yx}=\left(\frac{\partial^2\psi}{\partial y^2}-\delta^2\frac{\partial^2\psi}{\partial x^2}\right)+\alpha_1\left[-\delta^3\frac{\partial\psi}{\partial y}\frac{\partial^3\psi}{\partial x^3} +\delta\frac{\partial\psi}{\partial y}\frac{\partial^3\psi}{\partial x\partial y^2}+\delta^3\frac{\partial\psi}{\partial x}\frac{\partial^3\psi}{\partial x^2\partial y}-\delta\frac{\partial\psi}{\partial x}\frac{\partial^3\psi}{\partial y^3} +2\delta\frac{\partial^2\psi}{\partial y^2}\frac{\partial^2\psi}{\partial x\partial y}+2\delta^3\frac{\partial^2\psi}{\partial x^2}\frac{\partial^2\psi}{\partial x\partial y}\right] \quad (20)$$

$$S_{yy}=-2\delta\frac{\partial^2\psi}{\partial x\partial y}+\alpha_1\left[-2\delta^2\frac{\partial\psi}{\partial y}\frac{\partial^3\psi}{\partial x^2\partial y} +2\delta^2\frac{\partial\psi}{\partial x}\frac{\partial^3\psi}{\partial x\partial y^2}+4\delta^2\left(\frac{\partial^2\psi}{\partial x\partial y}\right)^2-2\delta^2\frac{\partial^2\psi}{\partial x^2}\frac{\partial^2\psi}{\partial y^2} +2\left(\frac{\partial^2\psi}{\partial y^2}\right)^2\right]+\alpha_2\left[4\delta^2\left(\frac{\partial^2\psi}{\partial x\partial y}\right)^2+\left(\frac{\partial^2\psi}{\partial y^2}\right)^2 +\delta^4\left(\frac{\partial^2\psi}{\partial x^2}\right)^2-2\delta^2\frac{\partial^2\psi}{\partial x^2}\frac{\partial^2\psi}{\partial y^2}\right] \quad (21)$$

The corresponding dimensionless boundary conditions are

$$\psi = \frac{F}{2}, \quad \frac{\partial \psi}{\partial y} = -1, \quad \theta = 1 \quad \text{at} \quad y = h_1 \tag{22}$$

$$\psi = -\frac{F}{2}, \quad \frac{\partial \psi}{\partial y} = -1, \quad \theta = 0 \quad \text{at} \quad y = h_2 \tag{23}$$

where F is the flux in the wave frame and a, b, d and ϕ satisfy the relation $a^2 + b^2 + 2ab\cos\phi \leq (1+d)^2$.

3. Rate of Volume Flow

In the laboratory frame, the dimensional volume flow rate is

$$Q = \int_{H_2}^{H_1} \bar{U}(\bar{X}, \bar{Y}, \bar{t})\, d\bar{Y}. \tag{24}$$

The above expression in wave frame becomes

$$q = \int_{h_2}^{h_1} \bar{u}(\bar{x}, \bar{y})\, d\bar{y}. \tag{25}$$

From Eq.s (7), (24) and (25), we can write

$$Q = q + ch_1 - ch_2. \tag{26}$$

The average volume flow rate over one period $\left(T = \frac{\lambda}{c}\right)$ of the peristaltic wave is defined as

$$\bar{Q} = \frac{1}{T}\int_0^T Q dt \tag{27}$$

Using Eq.(26) into Eq.(27) and then integrating, yields

$$\bar{Q} = q + cd_1 + cd_2 \tag{28}$$

We define the dimensionless time-mean flows Θ and F respectively, in the laboratory and wave frame as

$$\Theta = \frac{\bar{Q}}{cd_1} \quad \text{and} \quad F = \frac{q}{cd_1}, \tag{29}$$

From Eq.(28), we obtain

$$\Theta = F + 1 + d \tag{30}$$

and

$$F = \int_{h_2}^{h_1} \frac{\partial \psi}{\partial y} dy = \psi(h_1(x)) - \psi(h_2(x)) \tag{31}$$

where

$$h_1(x) = 1 + a\cos(2\pi x),$$
$$h_2(x) = -d - b\cos(2\pi x + \phi) \tag{32}$$

4. Perturbation Solution

Since the Eq.s (16)-(18) are highly non-linear partial differential equations, the exact solutions are not amenable. Therefore, we use regular perturbation method to find the approximate solution using the pertarbation parameter δ. For perturbation solution, we express ψ, θ and $\frac{\partial p}{\partial x}$ as

$$\psi = \psi_0 + \delta\psi_1 + O(\delta^2) \tag{33}$$

$$\theta = \theta_0 + \delta\theta_1 + O(\delta^2) \tag{34}$$

$$\frac{\partial p}{\partial x} = \frac{\partial p_0}{\partial x} + \delta\frac{\partial p_1}{\partial x} + O(\delta^2) \tag{35}$$

Substituting Eq.s (33)-(35) in Eq.s(16)-(23), and comparing the like power of δ, we get the zeroth order and first order systems. Solving these systems with the corresponding boundary conditions, the expressions of the stream function ψ, the temperature θ and the pressure gradient $\frac{\partial p}{\partial x}$ are given by

$$\begin{aligned}\psi = \; & C_1\cosh(Ry) + C_2\sinh(Ry) + C_3y^3 + C_4y^2 \\ & + C_5y + C_6 + \delta[G_1y^3\sinh(Ry) \\ & + G_2y^3\cosh(Ry) + G_3y^2\sinh(Ry) \\ & + G_4y^2\cosh(Ry) + G_5y\sinh(Ry) \\ & + G_6y\cosh(Ry) + G_7\cosh(2Ry) \\ & + G_8\sinh(Ry) + G_9\cosh(Ry) + G_{10}y^6 \\ & + G_{11}y^5 + G_{12}y^4 + G_{13}y^3 + G_{14}y^2 \\ & + G_{15}y + G_{16}]\end{aligned} \tag{36}$$

$$\begin{aligned}\theta = \; & -\frac{\beta}{2}y^2 + A_1y + A_2 + \delta[D_{29}y\sinh(Ry) \\ & + D_{30}y\cosh(Ry) + D_{31}\sinh(Ry) \\ & + D_{32}\cosh(Ry) + D_{33}y^5 + D_{34}y^4 \\ & + D_{35}y^3 + D_{36}y^2 + E_1y + E_2]\end{aligned} \tag{37}$$

$$\begin{aligned}\frac{\partial p}{\partial x} = \; & I_1y^2 + I_2y + I_3 + \delta[J_1y^2\sinh(Ry) \\ & + J_2y^2\cosh(Ry) + J_3y\sinh(Ry) \\ & + J_4y\cosh(Ry) + J_5\sinh(Ry) \\ & + J_6\cosh(Ry) + J_7\sinh^2(Ry) \\ & + J_8\cosh^2(Ry) + J_9\sinh(Ry)\cosh(Ry) \\ & + J_{10}\sinh(2Ry) + J_{11}y^5 + J_{12}y^4 + J_{13}y^3 \\ & + J_{14}y^2 + J_{15}y + J_{16}]\end{aligned} \tag{38}$$

The non-dimensional expression for the pressure difference per wavelength is given as follows

$$\Delta p_\lambda = \int_0^1 \left(\frac{dp}{dx}\right) dx. \tag{39}$$

The frictional forces at $y = h_1$ and $y = h_2$ denoted by $F_{\lambda 1}$ and $F_{\lambda 2}$ respectively are given as (Saleem and Haider 2014)

$$F_{\lambda 1} = \int_0^1 h_1^2 \left(-\frac{dp}{dx}\right) dx, \tag{40}$$

$$F_{\lambda 2} = \int_0^1 h_2^2 \left(-\frac{dp}{dx}\right) dx \tag{41}$$

The coefficients of the heat transfer Z_{h_1} and Z_{h_2} at the walls $y = h_1$ and $y = h_2$ respectively, are given by (Mehmood *et al.* 2012)

$$Z_{h_1} = \frac{\partial h_1}{\partial x}\frac{\partial \theta}{\partial y}, \tag{42}$$

$$Z_{h_2} = \frac{\partial h_2}{\partial x}\frac{\partial \theta}{\partial y} \tag{43}$$

After using Eq.(37) in the Eq.s(42)-(43), the expressions for heat transfer coefficients are

$$\begin{aligned} Z_{h_1} = {} & D_1[-\frac{\beta y}{2} + A_1 + \delta(RD_{29} y\cosh(Ry) \\ & + RD_{30} y\sinh(Ry) + (D_{29} + RD_{32})\sinh(Ry) \\ & + (D_{30} + RD_{31})\cosh(Ry) + 5D_{33}y^4 \\ & + 4D_{34}y^3 + 3D_{35}y^2 + 2D_{36}y + E_1)], \end{aligned} \tag{44}$$

$$\begin{aligned} Z_{h_2} = {} & D_2[-\frac{\beta y}{2} + A_1 + \delta(RD_{29} y\cosh(Ry) \\ & + RD_{30} y\sinh(Ry) + (D_{29} + RD_{32})\sinh(Ry) \\ & + (D_{30} + RD_{31})\cosh(Ry) + 5D_{33}y^4 \\ & + 4D_{34}y^3 + 3D_{35}y^2 + 2D_{36}y + E_1)] \end{aligned} \tag{45}$$

The expression for pressure gradient is not amicable for integration with respect to x. Hence, the pressure difference and frictional forces are computed numerically.

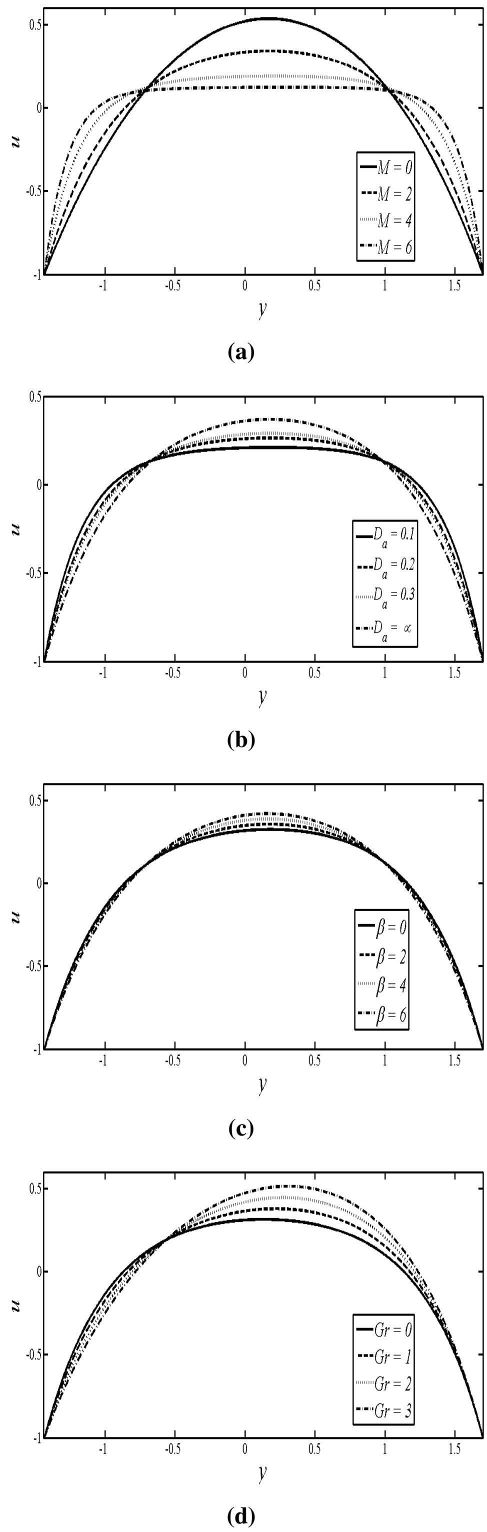

Fig. 2. Velocity profiles for (a) $x = 1$, $a = 0.7$, $b = 0.5$, $d = 1$, $Gr = 0.4$, $\delta = 0.0001$, $\Theta = 2$, $\alpha_1 = 0.5$, $D_a = 1$, $Re = 0.1$, $Pr = 0.5$, $\phi = \pi/6$, **and** $\beta = 1$; **(b)** $x = 1$, $a = 0.7$, $b = 0.5$, $d = 1$, $Gr = 0.4$, $\delta = 0.0001$, $\Theta = 2$, $\alpha_1 = 0.5$, $Re = 0.1$, $Pr = 0.5$, $\phi = \pi/6$, $M = 2$ **and** $\beta = 1$; **(c)** $x = 1$, $a = 0.7$, $b = 0.5$, $d = 1$, $Gr = 0.4$, $\delta = 0.0001$, $\Theta = 2$, $\alpha_1 = 0.5$, $D_a = 1$, $Re = 0.1$, $Pr = 0.5$, $\phi = \pi/6$ **and** $M = 2$; **(d)** $x = 1$, $a = 0.7$, $b = 0.5$, $d = 1$, $\delta = 0.0001$, $\Theta = 2$, $\alpha_1 = 0.5$, $D_a = 1$, $Re = 0.1$, $Pr = 0.5$, $\phi = \pi/6$, $M = 2$ **and** $\beta = 1$.

5. Results and Discussion

The main purpose of this section is to describe the effects of the different parameters on the streamlines, velocity, pressure gradient, frictional force and pressure difference. Numerical integration is performed over the domain $[0,1]$ for pressure difference and frictional force. The temperature profiles and the heat transfer coefficient are also analyzed for the various parameters. The results are presented graphically.

The variations of velocity for different values of Hartmann number M, Darcy number D_a, heat generation parameter β and Grashof number Gr are presented in the Fig.s2(a)-2(d). It is observed from figure 2(a) that, the velocity increases near the boundaries and decreases in the middle of the channel as Hartmann number M increases. From Fig.s2(b)-2(c), it is clear that, with increasing of Darcy number D_a and heat generation parameter β, the velocity decreases near the channel walls and increases near the middle of the channel. It is depicted from Fig.2(d) that, with the increase in Grashof number Gr, the velocity profile decreases in the left side of the channel, while it increases in the right side of the channel. Figures 3(a)-3(d) show that for $x \in [0,0.2]$ and $x \in [0.7.1]$, the pressure gradient is small, that is, the flow can easily pass without imposition of large pressure gradient and in remaining part of the channel, the pressure gradient is large, that is, it requires a large pressure gradient to maintain the given volume flow rate. Moreover, from Fig.3(a), the pressure gradient increases with an increase in Hartmann number M, in the wider part of the channel and decreases in the narrow part of the channel. The behavior is opposite for Darcy number D_a to that of Hartmann number M (see Fig.3(b)). It is noticed from the Fig.3(c) that, pressure gradient is increasing function of heat generation parameter β. It is depicted from figure 3(d) that, with the increasing of phase difference ϕ the pressure gradient decreases in the wider part of the channel and increases in the narrow part of the channel. Moreover, the narrow region in the channel is shifting to the left with an increase in ϕ. The pressure gradient for various wave forms are displayed in Fig. 4. It is observed from Fig.s 4(a)-4(d) that, pressure gradient increases with increasing volume flow rate. The pressure gradient is small in the wider part of the channel and large in the narrow part of the channel showing that, in the narrow part of the channel, more pressure gradient is required to push the fluid as compared with the wider part of the channel in all the wave shapes.

Figure 5 is prepared for pressure difference Δp_λ

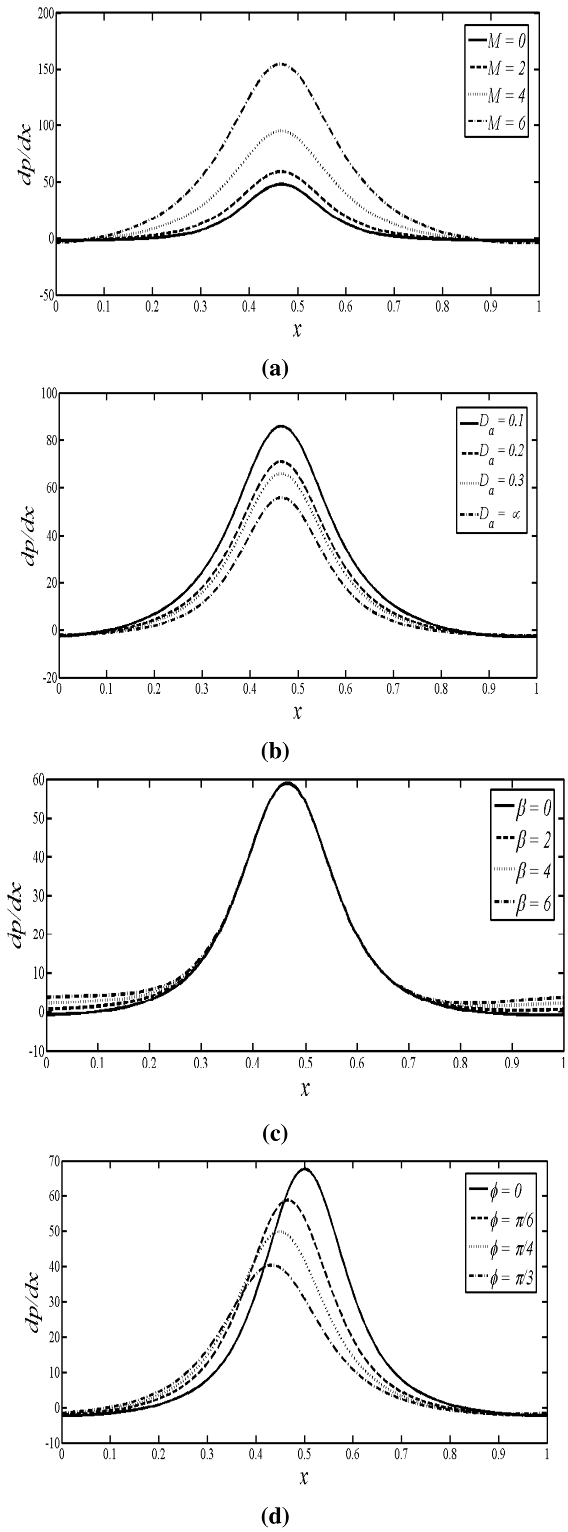

Fig. 3. Pressure gradient for (a) $y=0$, $a=0.7$, $b=0.5$, $d=1$, $Gr=0.4$, $\delta=0.0001$, $\Theta=-1$, $\alpha_1=0.5$, $D_a=1$, $Re=0.1$, $Pr=0.5$, $\phi=\pi/6$, **and** $\beta=1$; **(b)** $y=0$, $a=0.7$, $b=0.5$, $d=1$, $Gr=0.4$, $\delta=0.0001$, $\Theta=-1$, $\alpha_1=0.5$, $Re=0.1$, $Pr=0.5$, $\phi=\pi/6$, $M=2$ **and** $\beta=1$; **(c)** $y=0$, $a=0.7$, $b=0.5$, $d=1$, $Gr=0.4$, $\delta=0.0001$, $\Theta=-1$, $\alpha_1=0.5$, $D_a=1$, $Re=0.1$, $Pr=0.5$, $\phi=\pi/6$ **and** $M=2$; **(d)** $y=0$, $a=0.7$, $b=0.5$, $d=1$, $Gr=0.4$, $\delta=0.0001$, $\Theta=-1$, $\alpha_1=0.5$, $D_a=1$, $Re=0.1$, $Pr=0.5$, $M=2$ **and** $\beta=1$.

against volume flow rate Θ for different values of M, D_a and β. It is observed from Fig.5(a) that, when $\Delta p > 0$ the pumping rate increases with the increasing of M, pumping rate coincides with each other for $\Delta p = 0$ and for $\Delta p < 0$ the pumping rate decreases with the increase in M. The behaviour opposite with Darcy number D_a to that of Hartmann number M (see Fig.5(b)). From Fig.5(c), it is seen that with increase in β, the pressure difference increases. It is noted from figure 6 that, the frictional forces at the walls are acting opposite behaviour of pressure difference.

Figure 7 plots the temperature profiles for various values of flow parameters. Figures 7(a)-7(c) show that the temperature increases as heat generation parameter β, Grashof number Gr and the volume flow rate Θ increases. Figure 7(d) depicts that θ decreases by increasing Hartmann number M. Figure 8 is prepared to study the role of different parameters on the heat transfer coefficient at the wall $y = h_1$. Figure 8(a) shows that the absolute value of heat transfer coefficient increases by increasing heat generation parameter β. It is observed from the Fig.s8(b)-8(c) that, heat transfer coefficient increases with increasing of Grashof number Gr and the volume flow rate Θ. The situation is reversed with the increasing of Hartmann number M (see Fig.8(d)) to that of Grashof number Gr and the volume flow rate Θ. The trapping phenomena is discussed for different values of heat generation parameter β and Darcy number D_a for both symmetric and asymmetric channels in the Fig.s9-10. The streamlines (a), (b) are for symmetric channel while the streamlines (c), (d) are for asymmetric channel. It is observed from Fig.s9-10 that, the size of the trapped bolus increases with increase in heat generation parameter β and Darcy number D_a for both symmetric and asymmetric channels. Moreover, the effect of phase shift ϕ on trapping with the same amplitudes are shown in these figures. It is found that the bolus decreases and moves towards up with the increase of phase difference ϕ.

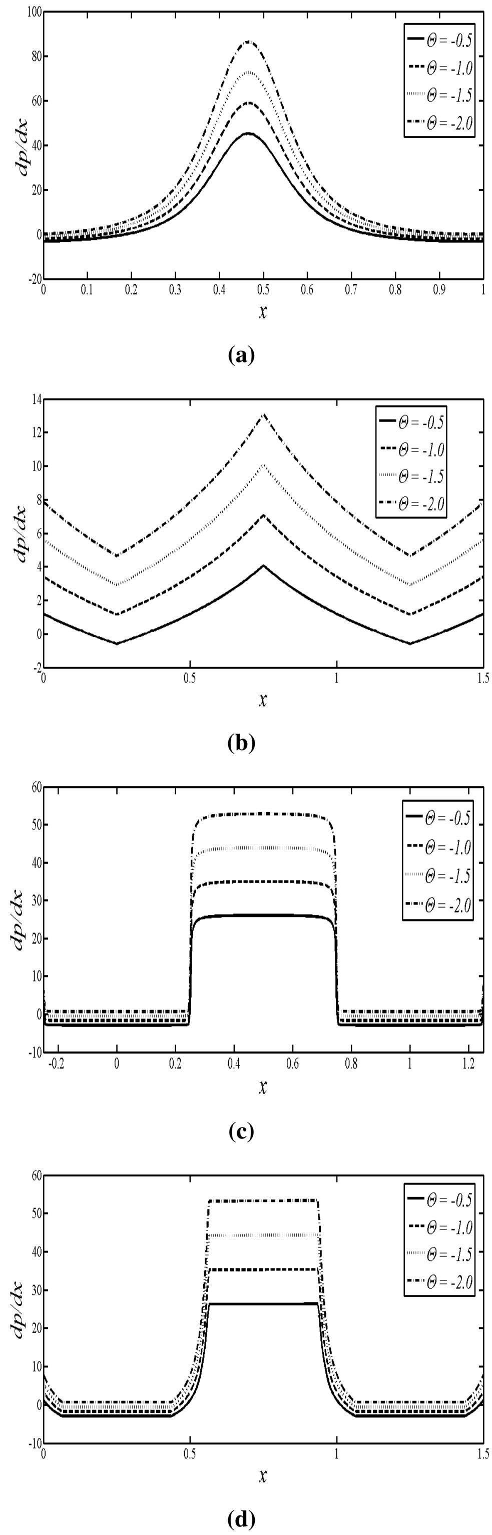

Fig. 4. Pressure gradient for various wave forms when $y = 0$, $a = 0.5$, $b = 0.5$, $d = 1$, $Gr = 0.4$, $\delta = 0.0001$, $\alpha_1 = 0.5$, $D_a = 1$, $Re = 0.1$, $Pr = 0.5$, $\phi = 0$, $\beta = 1$ **and** $M = 2$.

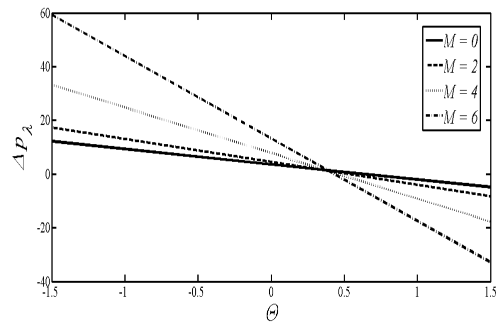

(a)

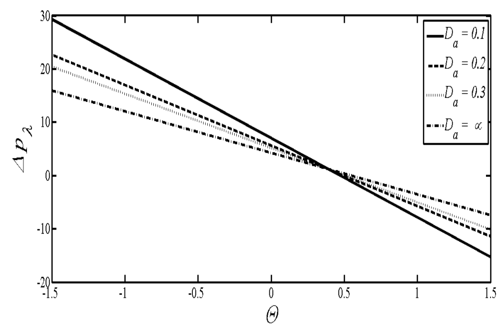

(b)

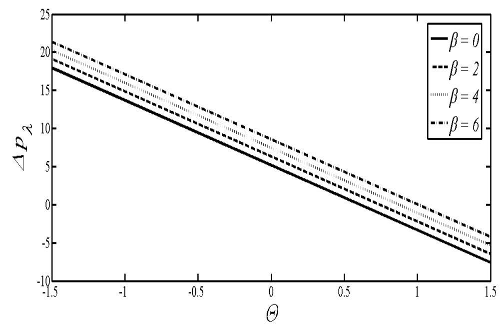

(c)

Fig. 5. Pressure difference for fixed values of (a) $y=0$, $a=0.7$, $b=0.5$, $d=1$, $Gr=0.4$, $\delta=0.0001$, $\Theta=-1$, $\alpha_1=0.5$, $D_a=1$, $Re=0.1$, $Pr=0.5$, $\phi=\pi/6$, **and** $\beta=1$; **(b)** $y=0$, $a=0.7$, $b=0.5$, $d=1$, $Gr=0.4$, $\delta=0.0001$, $\Theta=-1$, $\alpha_1=0.5$, $Re=0.1$, $Pr=0.5$, $\phi=\pi/6$, $M=2$ **and** $\beta=1$; **(c)** $y=0$, $a=0.7$, $b=0.5$, $d=1$, $Gr=0.4$, $\delta=0.0001$, $\Theta=-1$, $\alpha_1=0.5$, $D_a=1$, $Re=0.1$, $Pr=0.5$, $\phi=\pi/6$ **and** $M=2$.

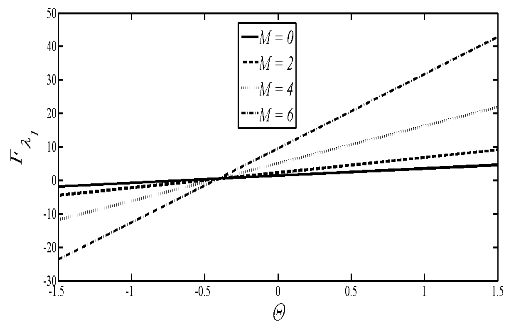

(a)

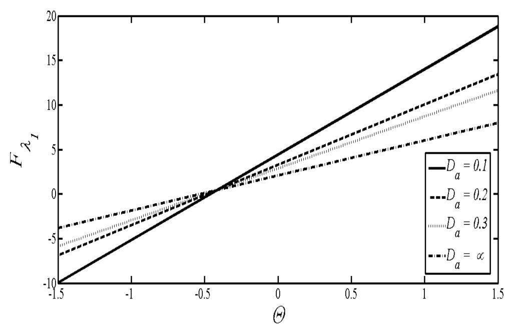

(b)

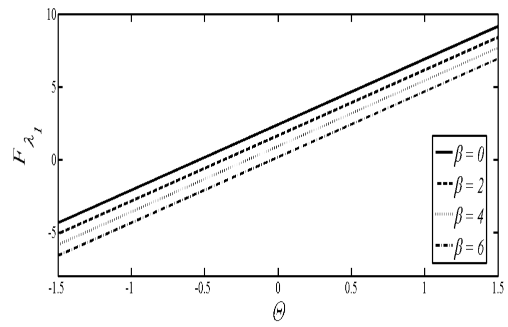

(c)

Fig. 6. Frictional force at the wall $y=h_1$ **for (a)** $a=0.7$, $b=0.5$, $d=1$, $Gr=0.4$, $\delta=0.0001$, $\Theta=-1$, $\alpha_1=0.5$, $D_a=1$, $Re=0.1$, $Pr=0.5$, $\phi=\pi/6$, **and** $\beta=1$; **(b)** $a=0.7$, $b=0.5$, $d=1$, $Gr=0.4$, $\delta=0.0001$, $\Theta=-1$, $\alpha_1=0.5$, $Re=0.1$, $Pr=0.5$, $\phi=\pi/6$, $M=2$ **and** $\beta=1$; **(c)** $a=0.7$, $b=0.5$, $d=1$, $Gr=0.4$, $\delta=0.0001$, $\Theta=-1$, $\alpha_1=0.5$, $D_a=1$, $Re=0.1$, $Pr=0.5$, $\phi=\pi/6$ **and** $M=2$.

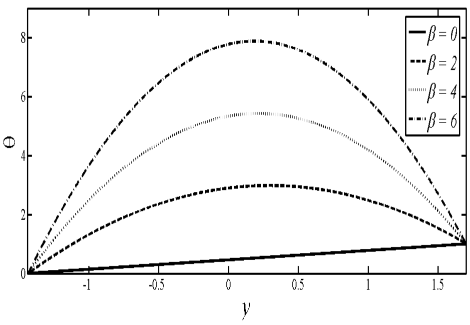

(a)

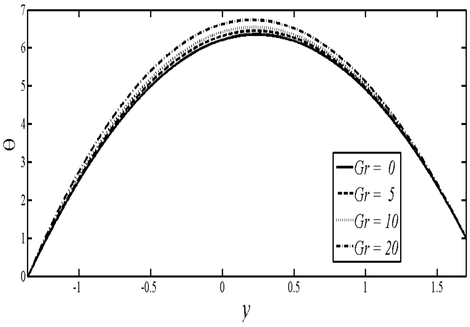

(b)

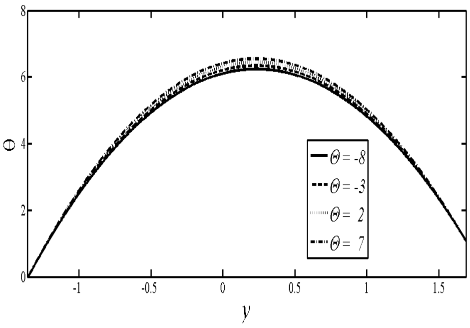

(c)

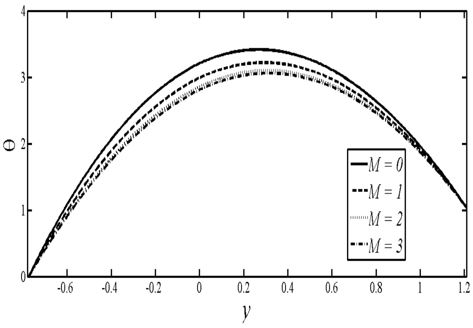

(d)

Fig. 7. Temperature profile for (a) $x = 1$, $a = 0.7$, $b = 0.5$, $d = 1$, $Gr = 5$, $\delta = 0.001$, $\Theta = 2$, $\alpha_1 = 0.2$, $D_a = 1$, $Re = 0.8$, $Pr = 0.8$, $\phi = \pi/4$ **and** $M = 2$; **(b)** $x = 1$, $a = 0.7$, $b = 0.5$, $d = 1$, $\delta = 0.001$, $\beta = 5$, $\Theta = 2$, $\alpha_1 = 0.2$, $D_a = 1$, $Re = 0.8$, $Pr = 0.8$, $\phi = \pi/4$ **and** $M = 2$; **(c)** $x = 1$, $a = 0.7$, $b = 0.5$, $d = 1$, $Gr = 5$, $\delta = 0.001$, $\beta = 5$, $\alpha_1 = 0.2$, $D_a = 1$, $Re = 0.8$, $Pr = 0.8$, $\phi = \pi/4$ **and** $M = 2$; **(d)** $x = 1$, $a = 0.7$, $b = 0.5$, $d = 1$, $Gr = 5$, $\delta = 0.001$, $\beta = 5$, $\Theta = 2$, $\alpha_1 = 0.2$, $D_a = 1$, $Re = 0.8$, $Pr = 0.8$ **and** $\phi = \pi/4$.

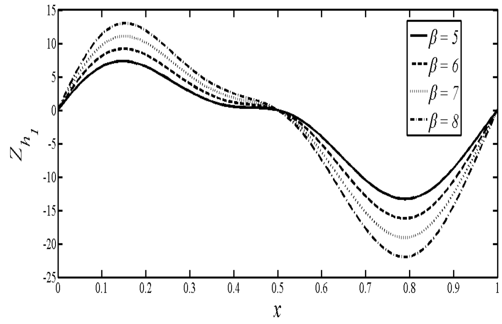

(a)

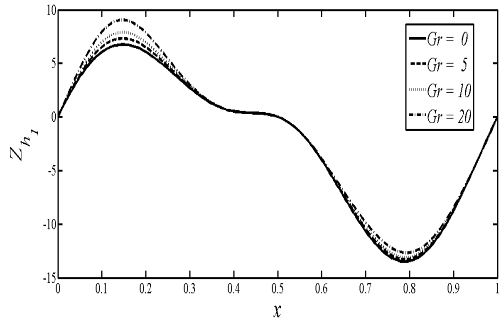

(b)

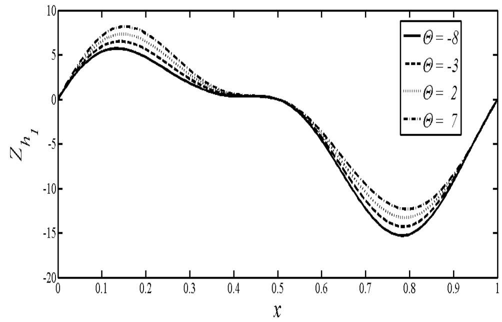

(c)

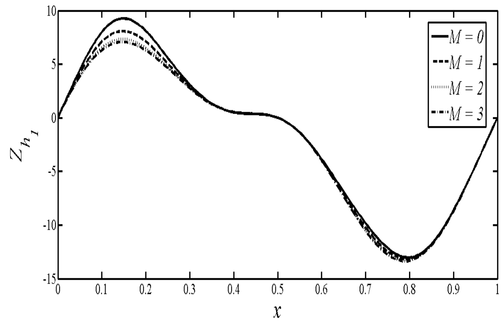

(d)

Fig. 8. Heat transfer coefficient at the wall $y = h_1$ **for (a)** $a = 0.7$, $b = 0.5$, $d = 1$, $Gr = 5$, $\delta = 0.001$, $\Theta = 2$, $\alpha_1 = 0.2$, $D_a = 1$, $Re = 0.8$, $Pr = 0.8$, $\phi = \pi/4$ **and** $M = 2$; **(b)** $a = 0.7$, $b = 0.5$, $d = 1$, $\delta = 0.001$, $\beta = 5$, $\Theta = 2$, $\alpha_1 = 0.2$, $D_a = 1$, $Re = 0.8$, $Pr = 0.8$, $\phi = \pi/4$ **and** $M = 2$; **(c)** $a = 0.7$, $b = 0.5$, $d = 1$, $Gr = 5$, $\delta = 0.001$, $\beta = 5$, $\alpha_1 = 0.2$, $D_a = 1$, $Re = 0.8$, $Pr = 0.8$, $\phi = \pi/4$ **and** $M = 2$; **(d)** $a = 0.7$, $b = 0.5$, $d = 1$, $Gr = 5$, $\delta = 0.001$, $\beta = 5$, $\Theta = 2$, $\alpha_1 = 0.2$, $D_a = 1$, $Re = 0.8$, $Pr = 0.8$ **and** $\phi = \pi/4$.

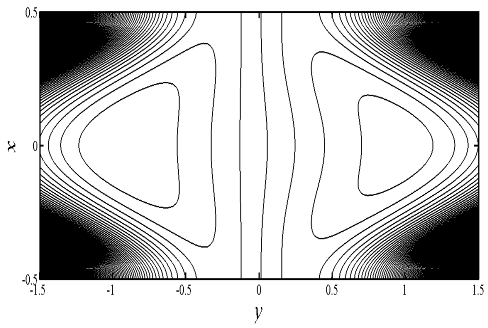

(a) $\beta = 0$, $\phi = 0$

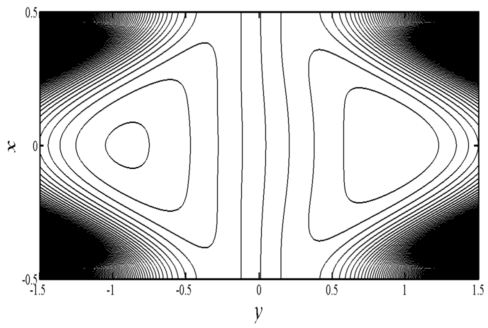

(b) $\beta = 5$, $\phi = 0$

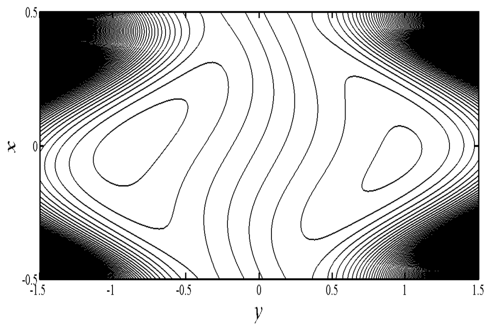

(c) $\beta = 0$, $\phi = \pi/6$

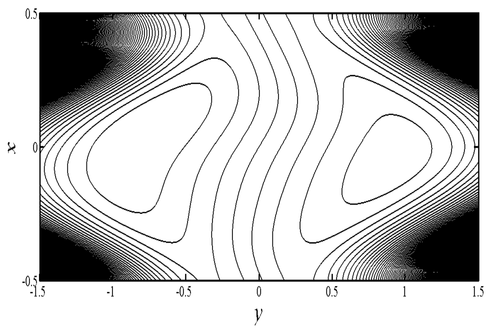

(d) $\beta = 5$, $\phi = \pi/6$

Fig. 9. Streamlines for $a = 0.5$, $b = 0.5$, $d = 1$, $Gr = 0.4$, $M = 2$, $\delta = 0.0001$, $\Theta = 2$, $\alpha_1 = 0.5$, $Re = 0.1$, $Pr = 0.5$ **and** $D_a = 1$.

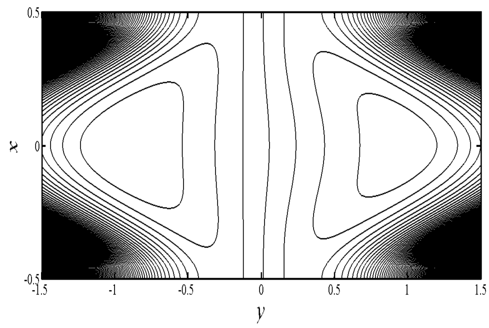

(a) $D_a = 1$, $\phi = 0$

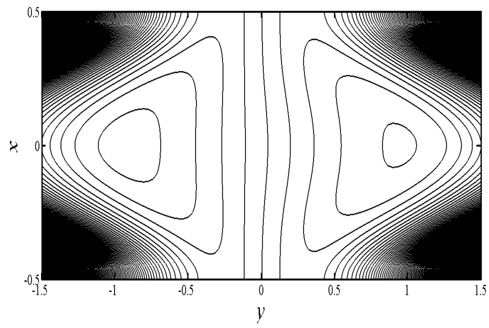

(b) $D_a \to \infty$, $\phi = 0$

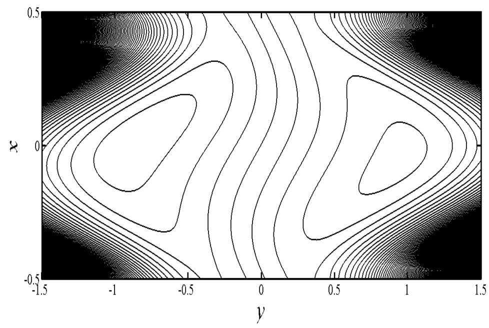

(c) $D_a = 1$, $\phi = \pi/6$

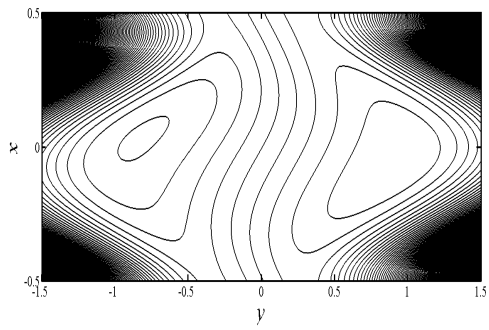

(d) $D_a \to \infty$, $\phi = \pi/6$

Fig. 10. Streamlines for $a = 0.5$, $b = 0.5$, $d = 1$, $Gr = 0.4$, $M = 2$, $\delta = 0.0001$, $\Theta = 2$, $\alpha_1 = 0.5$, $Re = 0.1$, $Pr = 0.5$ **and** $\beta = 1$.

6. Conclusions

The effects of heat transfer on the peristaltic flow of a magnetohydrodynamic second grade fluid through a porous medium in vertical symmetric and asymmetric channels are investigated. The velocity, frictional force, pumping, pressure gradient, temperature, trapping and heat transfer coefficient are examined for various fluid flow parameters. The main findings of the work are summarized as follows:

- The trapping bolus increases with increasing of heat generation parameter and Darcy number.
- The behaviour of velocity is qualitatively opposite for Hartmann number and porosity parameter.
- The pressure gradient for different wave forms is relatively small in the wider part of the channel and it is relatively large in the narrow part of the channel for given volume flow rate.
- The trapping bolus decreases and moves upward with an increase in phase difference.
- The heat generation parameter and Grashof number increases the temperature while Hartmann number decreases the temperature.
- The pressure difference and frictional forces have opposite behaviour on pumping.

Appendix

$$A_1 = \frac{1}{2(h_1-h_2)}\left(2+\beta(h_1^2-h_2^2)\right);$$

$$A_2 = \frac{1}{2}\left(2+\beta h_1^2-2A_1h_1\right); \quad R=\sqrt{M^2+\frac{1}{D_a}};$$

$$B_1 = \sinh(Rh_1)-\sinh(Rh_2);$$

$$B_2 = \cosh(Rh_1)-\cosh(Rh_2);$$

$$B_3 = \frac{Gr(h_1-h_2)}{2R^3}(\beta(h_1+h_2)-2A_1);$$

$$B_4 = \frac{R^3}{B_1}\left(B_1\cosh(Rh_1)-B_2\sinh(Rh_1)\right);$$

$$B_5 = \frac{B_3R^3\sinh(Rh_1)}{B_1}-\frac{Gr\beta Rh_1^2}{2}+GrA_1h_1 -\frac{Gr\beta}{R^2}+R^2;$$

$$B_6 = B_1-\frac{B_2^2}{B_1}-\frac{B_4(h_1-h_2)}{R^2};$$

$$C_1 = \frac{B_3-C_2B_2}{B_1};$$

$$C_2 = \frac{1}{B_6}\left(F-\frac{B_2B_3}{B_1}+\frac{Gr\beta(h_1^3-h_2^3)}{6R^2} +\frac{GrA_1(h_2^2-h_1^2)}{2R^2} +\left(\frac{Gr\beta}{R^4}+\frac{B_5}{R^2}\right)(h_1-h_2)\right);$$

$$C_3 = -\frac{Gr\beta}{6R^2}; \quad C_4=\frac{GrA_1}{2R^2};$$

$$C_5 = -\frac{Gr\beta}{R^4}-\frac{B_5+C_2B_4}{R^2};$$

$$C_6 = \frac{F}{2}-C_1\cosh(Rh_1)-C_2\sinh(Rh_1) +\frac{Gr\beta h_1^3}{6R^2}-\frac{GrA_1h_1^2}{2R^2}-C_5h_1;$$

$$I_1 = \frac{Gr\beta}{2}-6C_3R^2; \quad I_2=-A_1-2C_4R^2;$$

$$I_3 = 6C_3-A_2-(1+C_5)R^2;$$

$$D_1 = -2a\pi\sin(2\pi x); \quad D_2=2b\pi\sin(2\pi x+\phi);$$

$$D_3 = \frac{1}{2(h_1-h_2)^2}(2(D_2-D_1) +\beta(h_1-h_2)^2(2(D_1+D_2));$$

$$D_4 = \beta h_1D_1-A_1D_1-h_1D_3;$$

$$D_5 = R(D_1\cosh(Rh_1)-D_2\cosh(Rh_2));$$

$$D_6 = R(D_1\sinh(Rh_1)-D_2\sinh(Rh_2));$$

$$D_7 = \frac{Gr\beta}{R^3}(h_1D_1-h_2D_2)-\frac{Gr}{R^3}(A_1(D_1-D_2) +D_3(h_1-h_2));$$

$$D_8 = (RB_1D_1-D_6)\sinh(Rh_1) +(D_5-RB_2D_1)\cosh(Rh_1);$$

$$D_9 = B_1\cosh(Rh_1)-B_2\sinh(Rh_1);$$

$$D_{10} = \frac{1}{RD_9^2}(D_5D_9-B_1D_8);$$

$$D_{11} = \frac{1}{R^2B_1^2}(Gr\beta B_1^2D_1h_1-GrB_1^2(A_1D_1 +h_1D_3)+B_1^2D_{14}-B_1B_3D_1R^2\cosh(Rh_1) -B_1D_7R\sinh(Rh_1)+B_3D_5R\sinh(Rh_1));$$

$$D_{12} = \frac{R^3}{B_1^2}(B_1D_8-D_5D_9);$$

$$D_{13} = \frac{1}{B_1^2}(B_1B_3D_1R^4\cosh(Rh_1)+(B_1D_7R^3 -B_3D_5R^3)\sinh(Rh_1)) -Gr(\beta D_1h_1-A_1D_1-h_1D_3);$$

$$D_{14} = D_{13}+C_2D_{12}+B_4D_{18};$$

$$D_{15} = \frac{1}{R^2B_1^2}(B_1^2D_5R^2-2B_1B_2D_6R^2+B_2^2D_5R^2 -B_1^2B_4(D_1-D_2)-B_1^2D_{12}(h_1-h_2));$$

$$D_{16} = -\frac{1}{B_1^2}(B_1(B_2D_7+B_3D_6)-B_2B_3D_5) +\frac{Gr\beta}{6R^2}(3h_1^2D_1-3h_2^2D_2)$$

$$+\frac{Gr}{2R^2}[A_1(2h_2D_2-2h_1D_1)+D_3(h_2^2-h_1)^2]+\frac{Gr\beta}{R^4}(D_1-D_2)+\frac{1}{R^2}[B_5(D_1-D_2)+D_{13}(h_1-h_2)];$$

$$D_{17} = F-\frac{B_2B_3}{B_1}+\frac{Gr\beta}{6R^2}(h_1^3-h_2^3)+\frac{GrA_1}{2R^2}(h_2^2-h_1^2)+\left(\frac{Gr\beta}{R^4}+\frac{B_5}{R^2}\right)(h_1-h_2);$$

$$D_{18} = \frac{1}{B_6^2}(B_6D_{16}-D_{17}D_{15});$$

$$D_{19} = \frac{1}{B_1^2}(B_1D_7-B_1(C_2D_6+B_2D_{18})-D_5(B_3-C_2B_2));$$

$$D_{20} = R^2[RC_1D_1\sinh(Rh_1)+D_{19}\cosh(Rh_1)+RC_2D_1\cosh(Rh_1)+D_{18}\sinh(Rh_1)-\frac{Gr\beta}{2R^2}h_1^2D_1+\frac{Gr}{2R^2}(2h_1A_1D_1+h_1^2D_3)+C_5D_1-\frac{h_1D_{14}}{R^2}+\frac{Gr}{R^4}D_3];$$

$$D_{21} = RePr(RC_1D_3+\beta D_{18});$$

$$D_{22} = RePr(RC_2D_3+\beta D_{19});$$

$$D_{23} = RePr(RC_1D_4-A_1D_{18});$$

$$D_{24} = RePr(RC_2D_4-A_1D_{19});$$

$$D_{25} = RePr(3C_3D_3+\beta D_{37});$$

$$D_{26} = RePr(3C_3D_4+\beta D_{38}+2C_4D_3-A_1D_{37});$$

$$D_{27} = RePr(C_5D_3+\beta D_{39}+2C_4D_4-A_1D_{38});$$

$$D_{28} = RePr(RC_5D_4-A_1D_{39});\quad D_{29}=\frac{D_{21}}{R^2};$$

$$D_{30} = \frac{D_{22}}{R^2};\quad D_{31}=\frac{D_{23}}{R^2}-\frac{2D_{22}}{R^3};$$

$$D_{32} = \frac{D_{24}}{R^2}-\frac{2D_{21}}{R^3};\quad D_{33}=\frac{D_{25}}{20};\quad D_{34}=\frac{D_{26}}{12};$$

$$D_{35} = \frac{D_{27}}{6};\quad D_{36}=\frac{D_{28}}{2};\quad D_{37}=\frac{GrD_3}{2R^2};$$

$$D_{38} = -\frac{D_{14}}{R^2};\quad D_{39}=\frac{GrD_3}{R^4}-\frac{D_{20}}{R^2};$$

$$E_1 = \frac{1}{h_2-h_1}[D_{29}(h_1\sinh(Rh_1)-h_2\sinh(Rh_2))+D_{30}(h_1\cosh(Rh_1)-h_2\cosh(Rh_2))+D_{31}(\sinh(Rh_1)-\sinh(Rh_2))+D_{32}(\cosh(Rh_1)-\cosh(Rh_2))+D_{33}(h_1^5-h_2^5)+D_{34}(h_1^4-h_2^4)+D_{35}(h_1^3-h_2^3)+D_{36}(h_1^2-h_2^2)];$$

$$E_2 = -[D_{29}h_1\sinh(Rh_1)+D_{30}h_1\cosh(Rh_1)+D_{31}\sinh(Rh_1)+D_{32}\cosh(Rh_1)+D_{33}h_1^5+D_{34}h_1^4+D_{35}h_1^3+D_{36}h_1^2+E_1h_1];$$

$$E_3 = -\alpha_1\left[2R^3(C_1D_{19}+C_2D_{18})\right];$$

$$E_4 = -\alpha_1\left[2R^2C_4D_{19}+12C_3D_{18}R-C_2D_{38}R^3+2GrC_1D_3\right];$$

$$E_5 = -\alpha_1\left[2R^2C_4D_{18}+12C_3D_{19}R-C_1D_{38}R^3+2GrC_2D_3\right];$$

$$E_6 = -\alpha_1\left[R^2C_5D_{19}+\frac{GrC_2D_3}{R}-6C_3D_{19}-C_2D_{39}R^3+4C_4D_{18}R-2C_1D_{14}\right];$$

$$E_7 = -\alpha_1\left[R^2C_5D_{18}+\frac{GrC_1D_3}{R}-6C_3D_{18}-C_1D_{39}R^3+4C_4D_{19}R-2C_2D_{14}\right];$$

$$E_8 = -\alpha_1\left[2R^3C_1D_{18}\right];\quad E_9=-\alpha_1\left[2R^3C_1D_{19}\right];$$

$$E_{10} = -\alpha_1\left[3R^2C_3D_{19}-R^3C_2D_{37}\right];$$

$$E_{11} = -\alpha_1\left[3R^2C_3D_{18}-R^3C_1D_{37}\right];$$

$$E_{12} = -\alpha_1\left[\frac{15GrC_3D_3}{R^2}-6C_3D_{37}\right];$$

$$E_{13} = -\alpha_1\left[\frac{6GrC_4D_3}{R^2}-6C_3D_{38}-\frac{12C_3D_{14}}{R^2}\right];$$

$$E_{14} = -\alpha_1\left[\frac{GrC_5D_3}{R^2}-6C_3D_{39}-\frac{4C_4D_{14}}{R^2}\right];$$

$$E_{15} = R\left[2C_4D_{19}R^2-C_2D_{38}R^3\right];$$

$$E_{16} = R\left[2C_4D_{18}R^2-C_1D_{38}R^3\right];$$

$$E_{17} = R\left[C_5D_{19}R^2+\frac{GrC_2D_3}{R}-6C_3D_{19}-C_2D_{39}R^3\right];$$

$$E_{18} = R\left[C_5D_{18}R^2+\frac{GrC_1D_3}{R}-6C_3D_{18}-C_1D_{39}R^3\right];$$

$$E_{19} = R\left[3C_3D_{19}R^2-C_2D_{37}R^3\right];$$

$$E_{20} = R\left[3C_3D_{18}R^2-C_1D_{37}R^3\right];$$

$$E_{21} = R\left[\frac{3GrC_3D_3}{R^2}-6C_3D_{37}\right];$$

$$E_{22} = R\left[\frac{2GrC_4D_3}{R^2}-6C_3D_{38}\right];$$

$$E_{23} = R\left[\frac{GrC_5D_3}{R^2}-6C_3D_{39}\right];$$

$$E_{24} = 2\alpha[4C_1D_{19}R^5+4C_2D_{18}R^5];$$

$$E_{25} = 24\alpha C_3 D_{19} R^3 - \frac{GrD_{22}}{R};$$
$$E_{26} = 24\alpha C_3 D_{18} R^3 - \frac{GrD_{21}}{R};$$
$$E_{27} = 2\alpha[12C_3D_{18}R^2 + 4C_4D_{19}R^3 + 2RGrC_1D_3] + \frac{GrD_{21}}{R^2} - \frac{GrD_{24}}{R};$$
$$E_{28} = 2\alpha[12C_3D_{19}R^2 + 4C_4D_{18}R^3 + 2RGrC_2D_3] + \frac{GrD_{22}}{R^2} - \frac{GrD_{23}}{R};$$
$$E_{29} = 4\alpha[C_1D_{18}R^5 + C_2D_{19}R^5];$$
$$E_{30} = -\frac{GrD_{25}}{4}; \;\; E_{31} = -\frac{GrD_{26}}{3};$$
$$E_{32} = -\frac{GrD_{27}}{2}; \;\; E_{33} = -GrD_{28};$$
$$E_{34} = \frac{24\alpha GrC_3D_3}{R^2} - GrE_1; \;\; E_{35} = 4E_3R^2;$$
$$E_{36} = E_4R^2 + 4E_{11}R; \;\; E_{37} = E_5R^2 + 4E_{10}R;$$
$$E_{38} = 2E_5R + E_6R^2 + 2E_{10};$$
$$E_{39} = 2E_4R + E_7R^2 + 2E_{11};$$
$$E_{40} = 2E_8R^2 + 2E_9R^2; \;\; E_{41} = E_{10}R^2;$$
$$E_{42} = E_{11}R^2; \;\; E_{43} = 2E_{12};$$
$$F_1 = \frac{1}{8R^2}(E_{24} + E_{35} + 2E_{29} + 2E_{40});$$
$$F_2 = \frac{E_{29} + E_{41}}{R^2}; \;\; F_3 = \frac{E_{20} + E_{42}}{R^2};$$
$$F_4 = -\frac{4}{R^3}(E_{20} + E_{42}) + \frac{1}{R^2}(E_{15} + E_{26} + E_{36});$$
$$F_5 = -\frac{4}{R^3}(E_{20} + E_{42}) + \frac{1}{R^2}(E_{16} + E_{25} + E_{37});$$
$$F_6 = \frac{6}{R^4}(E_{29} + E_{41}) + \frac{2}{R^3}(E_{16} + E_{25} + E_{37}) + \frac{1}{R^2}(E_{17} + E_{28} + E_{38});$$
$$F_7 = \frac{6}{R^4}(E_{20} + E_{42}) + \frac{2}{R^3}(E_{15} + E_{26} + E_{36}) + \frac{1}{R^2}(E_{18} + E_{27} + E_{39});$$
$$F_8 = \frac{E_{30}}{30}; \;\; F_9 = \frac{E_{31}}{20}; \;\; F_{10} = \frac{E_{21} + E_{32}}{12};$$
$$F_{11} = \frac{E_{22} + E_{33}}{6};$$
$$F_{12} = \frac{1}{2}(E_{23} + E_{34} + E_{43}) - \frac{1}{4}(E_{24} + E_{35});$$
$$G_1 = \frac{F_2}{6R}; \;\; G_2 = \frac{F_3}{6R}; \;\; G_3 = \frac{F_4}{4R} - \frac{F_3}{4R^2};$$
$$G_4 = \frac{F_5}{4R} - \frac{F_2}{4R^2}; \;\; G_5 = \frac{F_2}{4R^3} - \frac{F_5}{4R^2} + \frac{F_6}{2R};$$
$$G_6 = \frac{F_3}{4R^3} - \frac{F_4}{4R^2} + \frac{F_7}{2R}; \;\; G_7 = \frac{F_1}{3R^2};$$
$$G_8 = -\frac{G_{20}}{G_{21}}; \;\; G_9 = \frac{1}{RB_1}\left[\frac{RB_2G_{20}}{G_{21}} - G_{17}\right];$$
$$G_{10} = -\frac{F_8}{R^2}; \;\; G_{11} = -\frac{F_9}{R^2};$$
$$G_{12} = -\frac{F_{10}}{R^2} - 30\frac{F_8}{R^4}; \;\; G_{13} = -\frac{F_{11}}{R^2} - 20\frac{F_9}{R^4};$$
$$G_{14} = -360\frac{F_8}{R^6} - 12\frac{F_{10}}{R^4} - \frac{F_{12}}{R^2};$$
$$G_{15} = -G_{18} + \frac{G_{20}}{G_{21}}R\cosh(Rh_1) + \frac{1}{B_1}\left[G_{17} - \frac{RB_2G_{20}}{G_{21}}\right]\sinh(Rh_1);$$
$$\begin{aligned} G_{16} = {} & -[G_1h_1^3\sinh(Rh_1) + G_2h_1^3\cosh(Rh_1) \\ & + G_3h_1^2\sinh(Rh_1) + G_4h_1^2\cosh(Rh_1) \\ & + G_5h_1\sinh(Rh_1) + G_6h_1\cosh(Rh_1) \\ & + G_7\cosh(2Rh_1) + G_{10}h_1^6 + G_{11}h_1^5 \\ & + G_{12}h_1^4 + G_{13}h_1^3 + G_{14}h_1^2 + G_{15}h]; \end{aligned}$$
$$\begin{aligned} G_{17} = {} & RG_2[h_1^3\sinh(Rh_1) - h_2^3\sinh(Rh_2)] \\ & + RG_1[h_1^3\cosh(Rh_1) - h_2^3\cosh(Rh_2)] \\ & + (3G_1 + RG_4)[h_1^2\sinh(Rh_1) - h_2^2\sinh(Rh_2)] \\ & + (3G_2 + RG_3)[h_1^2\cosh(Rh_1) - h_2^2\cosh(Rh_2)] \\ & + (2G_3 + RG_6)[h_1\sinh(Rh_1) - h_2\sinh(Rh_2)] \\ & + (2G_4 + RG_5)[h_1\cosh(Rh_1) - h_2\cosh(Rh_2)] \\ & + 2RG_7[\sinh(2Rh_1) - \sinh(2Rh_2)] \\ & + G_5[\sinh(Rh_1) - \sinh(Rh_2)] \\ & + G_6[\cosh(Rh_1) - \cosh(Rh_2)] \\ & + 6G_{10}(h_1^5 - h_2^5) + 5G_{11}(h_1^4 - h_2^4) \\ & + 4G_{12}(h_1^3 - h_2^3) + 3G_{13}(h_1^2 - h_2^2) \\ & + 2G_{14}(h_1 - h_2); \end{aligned}$$
$$\begin{aligned} G_{18} = {} & RG_2h_1^3\sinh(Rh_1) + RG_1h_1^3\cosh(Rh_1) \\ & + (3G_1 + RG_4)h_1^2\sinh(Rh_1) \\ & + (3G_2 + RG_3)h_1^2\cosh(Rh_1) \\ & + (2G_3 + RG_6)h_1\sinh(Rh_1) \\ & + (2G_4 + RG_5)h_1\cosh(Rh_1) \\ & + 2RG_7\sinh(2Rh_1) + G_5\sinh(Rh_1) \\ & + G_6\cosh(Rh_1) + 6G_{10}h_1^5 + 5G_{11}h_1^4 \\ & + 4G_{12}h_1^3 + 3G_{13}h_1^2 + 2G_{14}h_1; \end{aligned}$$
$$\begin{aligned} G_{19} = {} & G_1[h_1^3\sinh(Rh_1) - h_2^3\sinh(Rh_2)] \\ & + G_2[h_1^3\cosh(Rh_1) - h_2^3\cosh(Rh_2)] \\ & + G_3[h_1^2\sinh(Rh_1) - h_2^2\sinh(Rh_2)] \\ & + G_4[h_1^2\cosh(Rh_1) - h_2^2\cosh(Rh_2)] \\ & + G_5[h_1\sinh(Rh_1) - h_2\sinh(Rh_2)] \\ & + G_6[h_1\cosh(Rh_1) - h_2\cosh(Rh_2)] \\ & + G_7[\cosh(2Rh_1) - \cosh(2Rh_2)] \\ & + G_{10}(h_1^6 - h_2^6) + G_{11}(h_1^5 - h_2^5) \\ & + G_{12}(h_1^4 - h_2^4) + G_{13}(h_1^3 - h_2^3) \\ & + G_{14}(h_1^2 - h_2^2); \end{aligned}$$

$$G_{20} = G_{19} - \frac{B_2 G_{17}}{RB_1} + (h_1 - h_2)\left[\frac{G_{17}}{B_1}\sinh(Rh_1) - G_{18}\right];$$

$$G_{21} = B_1 - \frac{B_2^2}{B_1} + (h_1 - h_2)\left[\frac{RB_2}{B_1}\sinh(Rh_1) - R\cosh(Rh_1)\right];$$

$$\begin{aligned} G_{22} = {} & G_1 h_1^3 \sinh(Rh_1) + G_2 h_1^3 \cosh(Rh_1) \\ & + G_3 h_1^2 \sinh(Rh_1) + G_4 h_1^2 \cosh(Rh_1) \\ & + G_5 h_1 \sinh(Rh_1) + G_6 h_1 \cosh(Rh_1) \\ & + G_7 \cosh(2Rh_1) + G_{10} h_1^6 + G_{11} h_1^5 \\ & + G_{12} h_1^4 + G_{13} h_1^3 + G_{14} h_1^2 + G_{15} h; \end{aligned}$$

$$J_1 = 6G_1R^2 - E_{10}R - Re(3C_3D_{19}R - C_1D_{21}R^2);$$

$$J_2 = 6G_2R^2 - E_{11}R - Re(3C_3D_{18}R - C_1D_{21}R^2);$$

$$\begin{aligned} J_3 = {} & 12\alpha_2 C_3 D_{18} R^2 + 18G_2R + 4G_3R^2 - E_4R \\ & -2E_{11} + GrD_{29} - Re\left[\frac{GrC_1D_3}{R}\right. \\ & \left. +2C_4D_{19}R - 6C_3D_{18} - C_2D_{22}R^2\right]; \end{aligned}$$

$$\begin{aligned} J_4 = {} & 12\alpha_2 C_3 D_{19} R^2 + 18G_1R + 4G_4R^2 - E_5R \\ & -2E_{10} + GrD_{30} - Re\left[\frac{GrC_2D_3}{R}\right. \\ & \left. +2C_4D_{18}R - 6C_3D_{19} - C_1D_{22}R^2\right]; \end{aligned}$$

$$\begin{aligned} J_5 = {} & 4\alpha_2\left[C_4D_{18} + \frac{GrC_2D_3}{2R^2}\right]R^2 + 6G_1 + 2G_5R^2 \\ & +6G_4R - E_6R - E_5 + GrD_{31} + Re\left[\frac{C_1D_{14}}{R}\right. \\ & \left. -C_5D_{19}R + 2C_4D_{18} + C_2D_{23}R^2\right]; \end{aligned}$$

$$\begin{aligned} J_6 = {} & 4\alpha_2\left[C_4D_{19} + \frac{GrC_1D_3}{2R^2}\right]R^2 + 6G_2 + 2G_6R^2 \\ & +6G_3R - E_7R - E_4 + GrD_{32} + Re\left[\frac{C_2D_{14}}{R}\right. \\ & \left. -C_5D_{18}R + 2C_4D_{19} + C_1D_{23}R^2\right]; \end{aligned}$$

$$J_7 = 2\alpha_2 C_2 D_{18} R^4 - E_3R - Re[C_1D_{19}R^2 - C_2D_{18}R^2];$$

$$J_8 = 2\alpha_2 C_1 D_{19} R^4 - E_3R - Re[C_2D_{18}R^2 - C_1D_{19}R^2];$$

$$J_9 = 2\alpha_2 R^4(C_1D_{18} + C_2D_{19}) - 2R(E_8 + E_9);$$

$$J_{10} = 6G_7R^3; \quad J_{11} = -6G_{10}R^2 + GrD_{33};$$

$$J_{12} = -5G_{11}R^2 + GrD_{34};$$

$$J_{13} = 120G_{10} - 4G_{12}R^2 + GrD_{35} - Re\left[\frac{3GrC_3D_3}{R^2} - 6C_3D_{21}\right];$$

$$J_{14} = 60G_{11} - 3G_{13}R^2 + GrD_{36} - Re\left[\frac{2GrC_4D_3}{R^2} - \frac{3C_3D_{14}}{R^2} - 6C_3D_{22} - 2C_4D_{21}\right];$$

$$\begin{aligned} J_{15} = {} & \frac{12\alpha_2 GrC_4D_3}{R^2} - 2G_{14}R^2 + 24G_{12} + GrE_1 \\ & -2E_{12} - Re\left[\frac{GrC_5D_{13}}{R^2}\right. \\ & \left. -\frac{2C_4D_{14}}{R^2} - 6C_3D_{23} - 2C_4D_{22}\right]; \end{aligned}$$

$$\begin{aligned} J_{16} = {} & \frac{4\alpha_2 GrC_4D_3}{R^2} - G_{15}R^2 + 6G_{13} + GrE_2 \\ & -E_{13} - Re\left[-\frac{C_5D_{15}}{R^2} - 2C_4D_{23}\right]; \end{aligned}$$

REFERENCES

S. Nadeem and Noreen Sher Akbar, Influence of heat and mass transfer on the peristaltic flow of a Johnson Segalman fluid in a vertical asymmetric channel with induced MHD, Journal of the Taiwan Institute of Chemical Engineers 42 (2011) 58-66.

Manoranjan Mishra and Adabala Ramachandra Rao, Peristaltic transport of a Newtonian fluid in an asymmetric channel, Z. angew. Math. Phys. 54 (2003) 532-550.

Nasir Ali and Tasawar Hayat, Peristaltic flow of a micropolar fluid in an asymmetric channel, Computers and Mathematics with Applications 55 (2008) 589-608.

S. Noreen, A. Alsaedi and T. Hayat, Peristaltic flow of pseudoplastic fluid in an asymmetric channel, Journal of Applied Mechanics 79 (2012) 1-6.

P. Naga Rani and G. Sarojamma, Peristaltic transport of a Casson fluid in an asymmetric channel, Australasian Physical and Engineering Sciences in Medicine 27 (2004) 49-59.

B. V. Rathish kumar and K. B. Naidu, A numerical study of peristaltic flows, Computers and Fluids 24 (1995) 161-176.

T. Hayat, Ambreen Afsar, M. Khana and S. Asghar, Peristaltic transport of a third order fluid under the effect of a magnetic field, Computers and Mathematics with Applications 53 (2007) 1074-1087.

T. Hayat, Masood Khan, A.M. Siddiqui and S. Asghar, Non-linear peristaltic flow of a non-Newtonian fluid under effect of a magnetic field in a planar channel, Communications in Nonlinear Science and Numerical Simulation 12 (2007) 910-919.

M. Kothandapani and S. Srinivas, Peristaltic transport of a Jeffrey fluid under the effect of magnetic field in an asymmetric channel, International Journal of Non-Linear Mechanics 43 (2008) 915-924.

S. Nadeem and N. S. Akbar, Effects of induced magnetic field on peristaltic flow of Johnson-Segalman fluid in a vertical symmetric channel, Appl. Math. Mech. -Engl. Ed. 31(8) (2010) 969-978.

S. Nadeem and Safia Akram, Influence of inclined magnetic field on peristaltic flow of a Williamson fluid model in an inclined symmetric or asymmetric channel, Mathematical and Computer Modelling 52 (2010) 107-119.

Sohail Nadeem and Safia Akram, Peristaltic flow of a couple stress fluid under the effect of induced magnetic field in an asymmetric channel, Arch Appl Mech 81 (2011) 97-109.

Yongqi Wang, Nasir Ali and Tasawar Hayat, Peristaltic motion of a magnetohydrodynamic generalized second-order fluid in an asymmetric channel, Numerical Methods for Partial Differential Equations (2009) 415-435.

N. A. S. Afifi and N. S. Gad, Interaction of peristaltic flow with pulsatile magneto-fluid through a porous medium, Acta Mechanica 149 (2001) 229-237.

Y. Abd elmaboud and Kh.S. Mekheimer, Nonlinear peristaltic transport of a second-order fluid through a porous medium, Applied Mathematical Modelling 35 (2011) 2695-2710.

S. Nadeem and Safia Akram, Peristaltic flow of a Maxwell model through porous boundaries in a porous medium, Transp Porous Med 86 (2011) 895-909.

E.F. El-Shehawey and Saleh Z.A. Husseny, Peristaltic transport of a magneto-fluid with porous boundaries, Applied Mathematics and Computation 129 (2002) 421-440.

K. Vajravelu, S. Sreenadh, K. Rajanikanth and Changhoon Lee, Peristaltic transport of a Williamson fluid in asymmetric channels with permeable walls, Nonlinear Analysis: Real World Applications 13 (2012) 2804-2822.

Dharmendra Tripathi and O. Anwar Beg, A numerical study of oscillating peristaltic flow of generalized Maxwell viscoelastic fluids through a porous medium, Transp Porous Med 95 (2012) 337-348.

Sohail Nadeem and Safia Akram, Magnetohydrodynamic peristaltic flow of a hyperbolic tangent fluid in a vertical asymmetric channel with heat transfer, Acta Mech. Sin. 27(2) (2011) 237-250.

S. Nadeem and Noreen Sher Akbar, Effects of heat transfer on the peristaltic transport of MHD Newtonian fluid with variable viscosity: Application of Adomian decomposition method, Commun Nonlinear Sci Numer Simulat 14 (2009) 3844-3855.

T. Hayat, Najma Saleem, S. Asghar, Mohammed Shabab Alhothuali and Adnan Alhomaidan, Influence of induced magnetic field and heat transfer on peristaltic transport of a Carreau fluid, Commun Nonlinear Sci Numer Simulat 16 (2011) 3559-3577.

K. Vajravelu, S. Sreenadh, and P. Lakshminarayana, The influence of heat transfer on peristaltic transport of a Jeffrey fluid in a vertical porous stratum, Commun Nonlinear Sci Numer Simulat 16 (2011) 3107-3125.

S. Srinivas and M. Kothandapani, Peristaltic transport in an asymmetric channel with heat transfer - A note, International Communications in Heat and Mass Transfer 35 (2008) 514-522.

T. Hayat, Humaira Yasmina and Maryem Al-Yami, Soret and Dufour effects in peristaltic transport of physiological fluids with chemical reaction: A mathematical analysis, Computers and Fluids 89 (2014) 242-253.

O. U. Mehmood, N. Mustapha and S. Shafie, Heat transfer on peristaltic flow of fourth grade fluid in inclined asymmetric channel with partial slip, Appl. Math. Mech. - Engl. Ed. 33(10) (2012) 1313-1328.

Musharafa Saleem and Aun Haider, Heat and mass transfer on the peristaltic transport of non-Newtonian fluid with creeping flow, International Journal of Heat and Mass Transfer 68 (2014) 514-526.

Dharmendra Tripathi and O. Anwar Beg, A study on peristaltic flow of nanofluids: Application in drug delivery, systems, International Journal of Heat and Mass Transfer 70 (2014) 61-70.